

MAGNETIC FIELDS IN DISKS AND HALOS OF GALAXIES

Rainer Beck¹

Abstract. Radio synchrotron emission, its polarization and its Faraday rotation are powerful tools to study the strength and structure of interstellar magnetic fields. Total fields in gas-rich spiral arms and bars of nearby galaxies have strengths of 20–30 μG and are dynamically important. Ordered fields with spiral structure exist in grand-design, flocculent and even irregular galaxies. The strongest ordered fields of 5–10 μG are found in interarm regions, sometimes forming “magnetic spiral arms”. Faraday rotation sometimes reveals large-scale patterns which are signatures of coherent fields generated by dynamos, but in most galaxies the field has a complicated structure. – Magnetic fields with X-shaped patterns are observed in radio halos around edge-on galaxies. The synchrotron scale height allows to measure the mean outflow velocity, which seems to increase with the star-formation rate.

1 Introduction

Magnetic fields are a major agent in the interstellar medium. They contribute significantly to the total pressure which balances the gas disk against gravitation. They affect the dynamics of the turbulent interstellar medium (ISM) (de Avillez & Breitschwerdt 2005) and the gas flows in spiral arms (Gómez & Cox 2002). The shock strength in spiral density waves is decreased and structure formation is reduced in the presence of strong fields (Dobbs & Price 2008). The interstellar fields are closely connected to gas clouds. Magnetic fields stabilize gas clouds and reduce the star-formation efficiency to the observed low values (Price & Bate 2008, Vázquez-Semadeni *et al.* 2005). Cosmic rays accelerated in supernova remnants can provide the pressure to drive a *galactic outflow* and buoyant loops of magnetic fields via the *Parker instability* and can drive a dynamo (Hanasz *et al.* 2002, 2004). Understanding the interaction between the gas and the magnetic field is a key to understand the physics of galaxy disks and halos and the evolution of galaxies.

¹ Max-Planck-Institut für Radioastronomie, Auf dem Hügel 69, 53121 Bonn, Germany

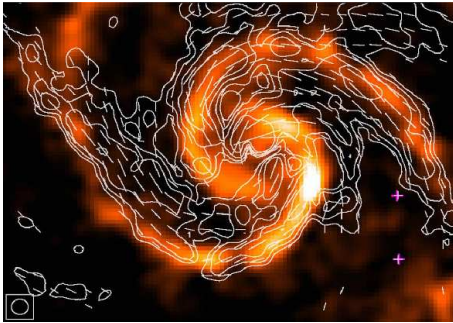


Fig. 1. Polarized radio emission (contours) and B -vectors of M 51 (8'' resolution), combined from observations at 6 cm wavelength with the VLA and Effelsberg telescopes (Fletcher *et al.*, in prep.). The background image shows the CO emission (Helfer *et al.* 2003) (Copyright: MPIfR Bonn).

2 Tools to measure interstellar magnetic fields

The intensity of *synchrotron emission* is a measure of the number density of cosmic-ray electrons in the relevant energy range and of the strength of the total magnetic field component in the sky plane. Polarized emission emerges from ordered fields. As polarization “vectors” are ambiguous by 180° , they cannot distinguish *regular fields*, with a constant direction within the telescope beam, from *anisotropic fields* which are generated from turbulent magnetic fields by compressing or shearing gas flows, with components frequently reversing their direction on small scales. Unpolarized synchrotron emission indicates *turbulent fields* with random directions.

The orientation of the observed B -vector is parallel to the field orientation at short radio wavelengths, so that the magnetic patterns of many galaxies could be mapped directly (Beck 2005). The orientation of the polarization vectors is changed in a magnetized thermal plasma by *Faraday rotation*. As the rotation angle is sensitive to the sign of the field direction, regular fields can give rise to Faraday rotation, while anisotropic and random fields do not. Faraday rotation measured from multi-wavelength observations allow to determine the strength and direction of the regular field component along the line of sight.

3 The radio–infrared correlation

The integrated flux densities of the total radio continuum emission at centimeter and decimeter wavelengths, which is mostly of nonthermal synchrotron origin, and far-infrared (FIR) emission of star-forming galaxies are tightly correlated over five orders of magnitude (Bell 2003). The correlation also holds for the local radio and far-IR or mid-IR intensities *within galaxies*: Strongest total synchrotron emission (tracing the total, mostly turbulent field) generally coincides with highest emission from dust and gas in the spiral arms. The highest correlation of all spectral ranges is between the total radio intensity and the mid-infrared dust emission, while the correlation with the cold gas is less tight (Frick *et al.* 2001). The radio–FIR correlation holds for large scales (Tabatabaei *et al.* 2007a), but breaks down for scales below about 50 pc (Hughes *et al.* 2006) and in radio halos, probably due to smoothing of the radio image by cosmic-ray propagation.

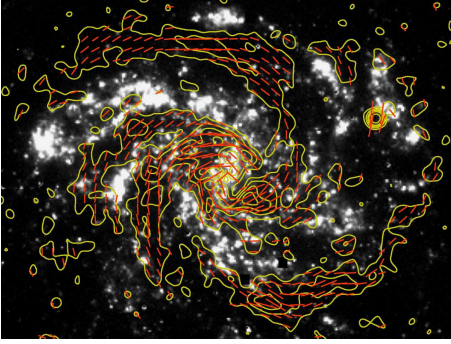


Fig. 2. Polarized radio emission (contours) and B -vectors of NGC 6946 (15'' resolution), combined from observations at 6 cm wavelength with the VLA and Effelsberg telescopes (Beck & Hoernes 1996). The background image shows the $H\alpha$ emission (Ferguson *et al.* 1998) (Copyright: MPIfR Bonn. Graphics: *Sterne und Weltraum*).

If the thermal and nonthermal radio components are separated, e.g. with help of $H\alpha$ and FIR data (Tabatabaei *et al.* 2007b), an almost perfect correlation is found between thermal radio and infrared intensities at all scales. The nonthermal–FIR correlation is less pronounced but highly significant, while the polarized synchrotron intensity, tracing the ordered field, is anticorrelated or not correlated with all tracers of star formation (Frick *et al.* 2001 and Fig. 2).

The radio–FIR correlation suggests that magnetic fields and star-formation processes are connected. If most nonthermal energy from cosmic-ray electrons (CRE) and most thermal energy from dust are emitted within a galaxy (“calorimeter”), a linear radio–FIR correlation for the integrated luminosities is obtained (Lisenfeld *et al.* 1996). Candidates for such galaxies are those with strong magnetic fields and high star-formation rates (SFR). However, the calorimeter model cannot explain the correlation within galaxies. In galaxies with low or moderate SFR and field strength, an almost linear correlation between the nonthermal radio luminosity and the FIR luminosity from warm dust is achieved by assuming coupling of magnetic fields to the gas clouds, energy equipartition between magnetic fields and cosmic rays, and a Schmidt law of star formation (Niklas & Beck 1997).

4 Equipartition field strengths

The radio–FIR correlation indicates that *equipartition* between the energy densities of the total magnetic field and the total cosmic rays is valid, at least on spatial scales larger than about 100 pc and on timescales of larger than the CRE acceleration time. Then the strength of the total magnetic field can be determined from the intensity of the total synchrotron emission, assuming a ratio K between the numbers of cosmic-ray protons and electrons (usually $K \simeq 100$). In regions where electrons lost already a significant fraction of their energy, K is > 100 and the standard value of 100 yields an underestimate (Beck & Krause 2005).

The typical average equipartition strength of the total magnetic field in spiral galaxies is about 10 μG . Radio-faint galaxies like M 31 and M 33 have weaker total magnetic fields of about 5 μG , like the Milky Way (Ferrière, this volume), while gas-rich galaxies with high star-formation rates, like M 51 (Fig. 1), M 83 and

NGC 6946, have total field strengths of 20–30 μG in their spiral arms. The degree of radio polarization within the spiral arms is only a few %; the field in the spiral arms is mostly tangled or randomly oriented within the telescope beam, which typically corresponds to a few 100 pc. The strongest total fields of 50–100 μG are found in starburst galaxies, like M 82 (Klein *et al.* 1988) and the “Antennae” NGC 4038/9 (Chyży & Beck 2004), and in nuclear starburst regions, like in the centers of NGC 1097 and other barred galaxies (Beck *et al.* 2005). In starburst galaxies the equipartition field strength per average gas surface density is much lower than in normal spirals. This indicates energy losses of the CRE, so that the equipartition field strength is underestimated (Thompson *et al.* 2006).

The mean energy densities of the magnetic field and of the cosmic rays in NGC 6946 and M 33 are $\simeq 10^{-11}$ erg cm $^{-3}$ and $\simeq 10^{-12}$ erg cm $^{-3}$, respectively (Beck 2007, Tabatabaei *et al.* 2008), about 10 times larger than that of the ionized gas, but similar to that of the turbulent gas motions across the star-forming disk. Another indication for dynamically important fields comes from the circumnuclear ring of NGC 1097 (Fig. 3, top right corner) where magnetic stress is strong to drive a mass inflow of about one solar mass of gas per year (Beck *et al.* 2005).

In case of energy equipartition, the scale length of the total field in the disk of galaxies is at least $(3 - \alpha)$ times larger than the synchrotron scale length of typically 4 kpc (where $\alpha \simeq -1$ is the synchrotron spectral index). The resulting value of $\simeq 16$ kpc is a lower limit because the CRE lose their energy with distance from the star-forming disk and the equipartition assumption yields too small values for the field strength. The galactic fields extend further out into intergalactic space than is observed. The same argument holds for the vertical extent of radio halos around galaxies (Fig. 4). As proposed by Battaner & Florido (2000), the magnetic field may affect galaxy rotation in the outermost parts of spiral galaxies.

5 Ordered and regular fields in galaxy disks

The ordered (regular and/or anisotropic) fields traced by the polarized synchrotron emission are generally strongest (10–15 μG) in the regions *between* the optical spiral arms, oriented parallel to the adjacent optical spiral arms. In some galaxies the field forms *magnetic arms* between the optical arms, like in NGC 6946 (Fig. 2). These are probably generated by a large-scale dynamo. In galaxies with strong density waves some of the ordered field is concentrated at the inner edge of the spiral arms, e.g. in M 51 (Patrikeev *et al.* 2006), but the arm–interarm contrast of the ordered field is small, much smaller than that of the random field.

The large-scale ordered magnetic field forms spiral patterns in almost every galaxy (Beck 2005), even in ring galaxies (Chyży & Buta 2008) and flocculent galaxies without an optical spiral structure (Soida *et al.* 2002). Hence, the field lines generally do *not* follow the (almost circular) gas flow and need dynamo action to obtain the required radial field components. Spiral fields are also observed in the central regions of galaxies and in circum-nuclear gas rings (Beck *et al.* 2005).

In galaxies with massive spiral arms (Fig. 1) or massive bars (Fig. 3) the ordered field is locally coupled to the shearing flow of the diffuse gas and is probably strong

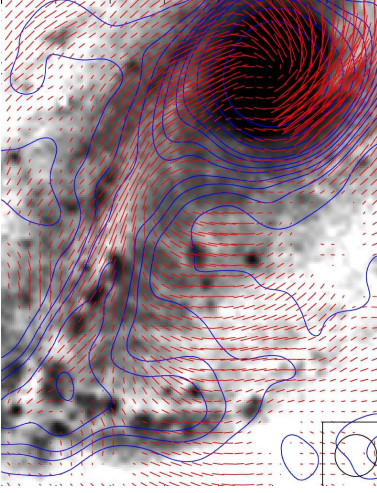


Fig. 3. Total radio emission (contours) and B -vectors of the barred galaxy NGC 1097 ($10''$ resolution), observed at 6 cm wavelength with the VLA (Beck *et al.* 2005). The background optical image is from Halton Arp (Copyright: MPIfR Bonn and Cerro Tololo Observatory).

enough to affect its flow (Beck *et al.* 2005). The polarization pattern in spiral arms and bars can be used as a tracer of shearing gas flows in the sky plane and hence complements spectroscopic measurements.

Regular (coherent) fields can be generated by the mean-field (or large-scale) *dynamo* (Beck *et al.* 1996). Dynamo fields are described by modes of different symmetry and can be identified from the pattern of Faraday rotation measures (RM) (Krause 1990, Elstner *et al.* 1992). The Andromeda galaxy M 31 hosts a dominating axisymmetric disk field (Fletcher *et al.* 2004). Other candidates for a dominating axisymmetric disk field are the nearby spiral IC 342 (Krause *et al.* 1989a) and the irregular Large Magellanic Cloud (LMC) (Gaensler *et al.* 2005). M 81 is a candidate for a bisymmetric field (Krause *et al.* 1989b), but the data quality is limited. The magnetic arms in NGC 6946 can be described by a superposition of two azimuthal dynamo modes which are phase shifted with respect to the optical arms (Beck 2007). However, in many observed galaxy disks no clear patterns of Faraday rotation were found. Either several dynamo modes are superimposed and cannot be distinguished with the limited sensitivity and resolution of present-day telescopes, or the timescale for the generation of large-scale modes is longer than the galaxy's lifetime. Dynamo models predict a rapid amplification of small-scale fields already in protogalaxies, while the generation of fully coherent large-scale fields takes several Gyrs, depending on the galaxy size (Arshakian *et al.* 2009). Furthermore, anisotropic fields dominate over dynamo modes if shearing gas flows are strong (see above).

A grid of Faraday rotation measurements of bright background sources allows to determine the field pattern in a foreground galaxy (Stepanov *et al.* 2008). This method can be applied to much larger distances than the analysis of RM of the polarized emission from a foreground galaxy itself. Faraday rotation of QSO emission in distant, intervening galaxies revealed significant regular fields of several μG strength (Kronberg *et al.* 2008, Bernet, this volume).

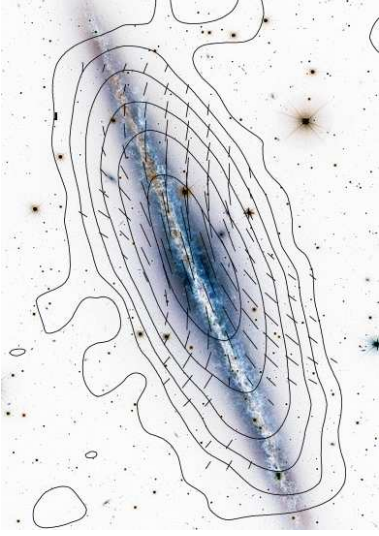


Fig. 4. Total radio emission and B -vectors of the edge-on spiral galaxy NGC 891 (84'' resolution), observed at 3.6 cm wavelength with the Effelsberg telescope (Krause 2008). The background optical image is from the *CFHT* (Copyright: MPIfR Bonn and *CFHT/Coelum*).

6 Magnetic fields in radio halos

Nearby galaxies seen edge-on generally show radio halos with a disk-parallel field near the disk plane (Dumke *et al.* 1995). Observations of edge-on galaxies like NGC 253 (Heesen *et al.* 2008), NGC 891 (Krause 2008, Fig. 4) and NGC 5775 (Tüllmann *et al.* 2000) revealed vertical field components in the halo, forming an X-shaped pattern. The field is probably transported into the halo by an outflow from the disk. Interestingly, a recent model for global outflows (however neglecting magnetic fields) shows an X-shaped velocity field (Dalla Vecchia & Schaye 2008).

The scale heights of radio halos of galaxies with different SFR are similar (Dumke & Krause 1998). The scale height decreases with increasing magnetic field strength (related to the SFR) due to synchrotron loss of the CRE, but this effect can be balanced by an outflow of gas and cosmic rays with a velocity increasing with SFR (Krause 2008, see also Koo, this volume). From the radio scale height and the lifetime of cosmic-ray electrons the outflow speed can be estimated; about 300 km/s was measured in the halo of NGC 253 (Heesen *et al.* 2008).

The exceptionally large radio halo around the irregular and interacting galaxy NGC 4631 reveals mostly radial fields in the inner region (Krause 2008). A few magnetic spurs could be resolved, connected to star-forming regions (Golla & Hummel 1994). The gravitational potential or the gravitational forces by the interaction may also play a role to determine the magnetic field structure in halos.

The mean-field dynamo generates large-scale helicity with a non-zero mean in each hemisphere. Total helicity is a conserved quantity, so that the dynamo is quenched by small-scale fields with opposite helicity unless these are removed by *outflows* which are essential for dynamo action (Shukurov *et al.* 2006).

Kinematical dynamo models including the velocity field of a global outflow predict field structures which are parallel to the plane in the inner disk and open

radially outwards (Brandenburg *et al.* 1993), similar to the observations. Dynamo models also predict large-scale RM patterns around edge-on galaxies. Indication for an antisymmetric vertical field was found so far in the halo of NGC 253 (Heesen *et al.*, in prep.). Improved models are needed, including the interplay between the gas flow and the magnetic field and the variation of the mean rotation velocity with height (Heald, this volume).

Interaction between galaxies or with the intergalactic medium imprints unique signatures onto magnetic fields in the outer disks and halos. The majority of galaxies in the Virgo cluster observed so far show asymmetric distributions of the polarized emission (Vollmer *et al.* 2007, Weżgowiec *et al.* 2007). Polarized radio emission is an excellent tracer of interactions and ram pressure.

7 Next-generation radio telescopes

The observation of magnetic fields is a major driver for most future radio telescopes. High-resolution, future deep observations at high frequencies with the Extended Very Large Array (EVLA) and the Square Kilometre Array (SKA) (Beck & Gaensler 2004) will directly show the detailed field structure and the interaction with the gas. The shape of the galaxy halos and their field structure allow to distinguish a global wind driven by star formation in the disk from galactic fountain or diffusion models. Faraday rotation measures trace regular fields and can test dynamo models. Forthcoming low-frequency radio telescopes like the Low Frequency Array (LOFAR) and the Murchison Widefield Array (MWA) will be suitable instruments to search for weak magnetic fields in outer galaxy disks and in halos (Beck 2008). Interaction between galaxies or with the intergalactic medium imprints unique signatures onto magnetic fields. As the decompression timescale of such fields is very long, they keep memory of events in the past and are best observable at low frequencies where the lifetime of the illuminating cosmic-ray electrons is sufficiently large.

References

- Arshakian, T.G., Beck, R., Krause, M. & Sokoloff, D. 2009, A&A, 494, 21
- Battaner, E. & Florido, E. 2000, Fund. Cosmic Phys., 21, 1
- Beck, R. 2005, in *"Cosmic Magnetic Fields"*, ed. R. Wielebinski & R. Beck (Berlin: Springer), p. 41
- Beck, R. 2007, A&A, 470, 539
- Beck, R. 2008, Rev. Mexicana AyA, in press, arXiv:0804.4594
- Beck, R. & Gaensler, B.M. 2004, New Astron. Rev., 48, 1289
- Beck, R. & Hoernes, P. 1996, Nature, 379, 47
- Beck, R. & Krause, M. 2005, Astron. Nachr., 326, 414
- Beck, R., Brandenburg, A., Moss, D., Shukurov, A. & Sokoloff, D. 1996, ARAA, 34, 155
- Beck, R., Fletcher, A., Shukurov, A. *et al.* 2005, A&A, 444, 739
- Bell, E.F. 2003, ApJ, 586, 794

- Brandenburg, A., Donner, K.J., Moss, D. *et al.*, 1993, A&A, 271, 36
- Chyży, K.T. & Beck, R. 2004, A&A, 417, 541
- Chyży, K.T. & Buta, R.J. 2008, ApJ, 677, L17
- Dalla Vecchia, C. & Schaye, J. 2008, MNRAS, 387, 1431
- de Avillez, M.A. & Breitschwerdt, D. 2005, A&A, 436, 585
- Dobbs, C.L. & Price, D.J. 2008, MNRAS, 383, 497
- Dumke, M. & Krause, M. 1998, in *"The Local Bubble and Beyond"*, ed. D. Breitschwerdt, M.J. Freyberg & J. Trümper (Berlin: Springer), p. 555
- Dumke, M., Krause, M., Wielebinski, R. & Klein, U. 1995, A&A, 302, 691
- Elstner, D., Meinel, R. & Beck, R. 1992, A&A Suppl., 94, 587
- Ferguson, A.M.N., Wyse, R.F.G., Gallagher, J.S. & Hunter, D.A. 1998, ApJ, 506, L19
- Fletcher, A., Berkhuijsen, E.M., Beck, R. & Shukurov, A. 2004, A&A, 414, 53
- Frick, P., Beck, R., Berkhuijsen, E.M. & Patrikeev, I. 2001, MNRAS, 327, 1145
- Gaensler, B.M., Haverkorn, M., Staveley-Smith, L. *et al.* 2005, Science, 307, 1610
- Golla, G. & Hummel, E. 1994, A&A, 284, 777
- Gómez, G.C. & Cox, D.P. 2002, ApJ, 580, 235
- Hanasz, M., Otmianowska-Mazur, K. & Lesch, H. 2002, A&A, 386, 347
- Hanasz, M., Kowal, G., Otmianowska-Mazur, K. & Lesch, H. 2004, ApJ, 605, L33
- Heesen, V., Beck, R., Krause, M. & Dettmar, R.-J. 2008, A&A, in press, arXiv:0812.0346
- Helfer, T.T., Thornley, M.D., Regan, M.W., *et al.* 2003, ApJS, 145, 259
- Hughes, A., Wong, T., Ekers, R. *et al.* 2006, MNRAS, 370, 363
- Klein, U., Wielebinski, R. & Morsi, H.W. 1988, A&A, 190, 41
- Krause, M. 1990, in *"Galactic and Intergalactic Magnetic Fields"*, ed. R. Beck, R. Wielebinski & P.P. Kronberg (Dordrecht: Kluwer), p. 187
- Krause, M. 2008, Rev. Mexicana AyA, in press, arXiv:0806.2060
- Krause, M., Hummel, E. & Beck, R. 1989a, A&A, 217, 4
- Krause, M., Beck, R. & Hummel, E. 1989b, A&A, 217, 17
- Kronberg, P.P., Bernet, M.L., Miniati, F. *et al.* 2008, ApJ, 676, 70
- Lisenfeld, U., Völk, H.J. & Xu, C. 1996, A&A, 314, 745
- Niklas, S. & Beck, R. 1997, A&A, 320, 54
- Patrikeev, I., Fletcher, A., Stepanov, R. *et al.* 2006, A&A, 458, 441
- Price, D.J. & Bate, M.R. 2008, MNRAS, 385, 1820
- Shukurov, A., Sokoloff, D., Subramanian, K. & Brandenburg, A. 2006, A&A, 448, L33
- Soida, M., Beck, R., Urbanik, M. & Braine, J. 2002, A&A, 394, 47
- Stepanov, R., Arshakian, T.G., Beck, R., Frick, P. & Krause, M. 2008, A&A, 480, 45
- Tabatabaei, F., Beck, R., Krause, M. *et al.* 2007a, A&A, 466, 509
- Tabatabaei, F., Beck, R., Krügel, E. *et al.* 2007b, A&A, 475, 133
- Tabatabaei, F., Krause, M., Fletcher, A. & Beck, R. 2008, A&A, 490, 1005
- Thompson, T.A., Quataert, E., Waxman, E., Murray, N. & Martin, C.L. 2006, ApJ, 645, 186
- Tüllmann, R., Dettmar, R.-J., Soida, M., Urbanik, M. & Rossa, J. 2000, A&A, 364, L36
- Vázquez-Semadeni, E., Kim, J. & Ballesteros-Paredes, J. 2005, ApJ, 630, L49
- Vollmer, B., Soida, M., Beck, R. *et al.*, 2007, A&A, 464, L37
- Weżgowiec, M., Urbanik, M., Vollmer, B. *et al.* 2007, A&A, 471, 93